Robust Control Pulses Design for Electron Shuttling in Solid-State Devices

Jun Zhang, *Senior Member, IEEE*, Loren Greenman, Xiaotian Deng, and K. Birgitta Whaley

***Abstract*— In this brief, we study robust pulse design for electron shuttling in solid-state devices. This is crucial for many practical applications of coherent quantum mechanical systems. Our objective is to design control pulses that can transport an electron along a chain of donors and that also make this process robust to parameter uncertainties. We formulate this problem here as a set of optimal control problems and derive explicit expressions for the gradients of the aggregate transfer fidelity. Numerical results for a donor chain of ionized phosphorus atoms in bulk silicon demonstrate the efficacy of our algorithm.**

***Index Terms*— Electron shuttling, pulses design, robust control.**

I. Introduction

RECENT years have witnessed the rapid advance of solid-state devices that take full advantage of coherent quantum-mechanical properties [1]. One particular application of such devices is quantum computation, which has attracted intensive research interest over the past 15 years. To implement these devices in practical applications, it is often desired to transfer the population between different spatial locations so that quantum information can be circulated and processed on a large scale.

This brief is focused on the robust coherent electron shuttling in solid-state devices with a 1-D array of quantum dots or donors so that the encoded quantum information can be communicated between distant qubits. Specifically, at the beginning of this procedure, an electron is localized at one end of the chain. Then, by applying some appropriate external control fields, we can shuttle the electron to the other end of the chain. Depending on the specific physical implementation, the control fields can be gate voltage [2] or tunable on-site energy [3].

Manuscript received October 6, 2013; revised November 28, 2013 and January 14, 2014; accepted February 22, 2014. Manuscript received in final form February 24, 2014. Date of publication March 18, 2014; date of current version October 15, 2014. The work of J. Zhang was supported in part by the Innovation Program of Shanghai Municipal Education Commission under Grant 11ZZ20, in part by the Shanghai Pujiang Program under Grant 11PJ1405800, in part by NSFC under Grant 61174086, in part by the State Key Laboratory of Precision Spectroscopy, in part by ECNU, China, and in part by the Project through SRF for ROCS SEM. The work of L. Greenman and K. B. Whaley was supported by NSA under Grant MOD713106A. Recommended by Associate Editor I. Petersen.

J. Zhang is with the Joint Institute of UM-SJTU, Shanghai Jiao Tong University, Shanghai 200240, China, and also with the Key Laboratory of System Control and Information Processing, Ministry of Education, Shanghai 200240, China (e-mail: zhangjun12@sjtu.edu.cn).

L. Greenman, X. Deng, and K. B. Whaley are with the Department of Chemistry, Berkeley Center for Quantum Information and Computation, University of California, Berkeley, CA 94720 USA (e-mail: loreng@berkeley.edu; dxt910922@berkeley.edu; whaley@berkeley.edu).

Color versions of one or more of the figures in this paper are available online at http://ieeexplore.ieee.org.

Digital Object Identifier 10.1109/TCST.2014.2308515

To achieve electron shuttling, Greentree *et al.* [2] have proposed to use coherent tunneling adiabatic passage (CTAP) pulses for population transfer, which is a solid-state version of the well-known stimulated Raman adiabatic passage in quantum optics [4]. The current authors have applied Lie–Poisson reduction to derive the dynamics of the optimal control with the removal of the adiabatic condition and accomplish the quantum state transfer with complete fidelity between spatial locations without any restriction to long-pulse durations [5].

In many experiments, it is inevitable that some physical parameters are not precisely known although we may have confidence that they lie in a certain range. In this situation, it is particularly important to design control pulses in a robust manner so that the electron shuttling process is insensitive to these parameter uncertainties. This is particularly important in solid-state quantum information processing implementations, such as impurity donors in Si [1], where the placement of the qubits is usually imprecise [6] and the interactions may be very sensitive to the distance between qubits [7]. In particular, the exchange interaction is exponentially sensitive to distance [8], and thus even in the absence of decoherence, it is essential to develop robust coherent control protocols when using this interaction as the basis for quantum logic.

Robust control of quantum mechanical systems has attracted extensive attention in both physics and control communities in recent years [9]–[16]. References [9]–[11] discussed robust control of quantum information processing and quantum systems. In [12], robust dynamical decoupling was developed to fight against a certain class of systematic implementation errors. Reference [13] studied robust steering in open-loop quantum systems, whereas [14] investigated robust stability and robust stabilization for quantum feedback networks. Recently, [15] and [16] discussed simultaneous control and stabilization for an ensemble of quantum systems.

The robustness of CTAP with respect to lateral straggle of the donors has been determined to be within the desired limits [17]; however, the robustness of the system with respect to deviations in the site energies [18] (as well as other effects of nonstandard geometries) is not as well studied. In this brief, we formulate the design of robust control pulses for electron shuttling as an optimal control problem. We discretize the uncertainty range and obtain a finite collection of state transfer problems, each of which takes a different value of the uncertainty parameter. Due to the maximal frequency constraints, we consider the control signals that can be expanded in Fourier expansion forms. The gradients of the aggregate fidelity with respect to the Fourier coefficients are then derived in an analytical form, which allows for effective implementations of

gradient types of optimization algorithms. Numerical studies demonstrate the efficiency of the algorithm with realistic physical parameters relevant to the electron shuttling between phosphorus dopant ions in silicon.

II. Problem Formulation

In this section, we provide a general mathematical description for electron shuttling in solid-state devices, together with the key associated mathematical background.

The underlying physics and potential applications of solid-state devices with qubits have been widely discussed in the physical community [2], [3], [19]. For a complete quantum description of the system under realistic conditions, it is necessary to employ the density operator ρ, which is a nonnegative definite Hermitian matrix with unit trace. The diagonal elements of the density operator correspond to the electron populations on each site. The dynamics of the density operator is determined by the Liouville–von Neumann equation (setting $\hbar = 1$)

$$\dot{\rho} = -[iH, \quad \rho] \tag{1}$$

where H is a traceless Hermitian matrix, which is termed the system Hamiltonian. As discussed earlier, we focus here on a triple donor system, but the development and solution shown here can be easily extended to devices with more donors. The term iH is defined on the Lie algebra $\mathfrak{su}(3)$, i.e., all the 3×3 skew-Hermitian matrices. In [2], an electron is moved between ends of a chain of ionized phosphorus dopants, for which the Hamiltonian is given by

$$H = \begin{bmatrix} 0 & -\Omega_{12} & 0 \\ -\Omega_{12} & \Delta & -\Omega_{23} \\ 0 & -\Omega_{23} & 0 \end{bmatrix}. \tag{2}$$

Here, Δ is the energy difference between eigenstates, and Ω_{12} and Ω_{23} are the coherent tunneling amplitudes between eigenstates.

Define a basis for $\mathfrak{su}(3)$ as

$$\begin{aligned} X_1 &= \begin{bmatrix} 0 & i & 0 \\ i & 0 & 0 \\ 0 & 0 & 0 \end{bmatrix}, \quad X_2 = \begin{bmatrix} 0 & 0 & 0 \\ 0 & 0 & i \\ 0 & i & 0 \end{bmatrix} \\ X_3 &= \begin{bmatrix} 0 & 0 & 1 \\ 0 & 0 & 0 \\ -1 & 0 & 0 \end{bmatrix}, \quad X_4 = \begin{bmatrix} 0 & 1 & 0 \\ -1 & 0 & 0 \\ 0 & 0 & 0 \end{bmatrix} \\ X_5 &= \begin{bmatrix} 0 & 0 & 0 \\ 0 & 0 & 1 \\ 0 & -1 & 0 \end{bmatrix}, \quad X_6 = \begin{bmatrix} 0 & 0 & i \\ 0 & 0 & 0 \\ i & 0 & 0 \end{bmatrix} \\ X_7 &= \begin{bmatrix} i & 0 & 0 \\ 0 & -i & 0 \\ 0 & 0 & 0 \end{bmatrix}, \quad X_8 = \tfrac{1}{\sqrt{3}} \begin{bmatrix} i & 0 & 0 \\ 0 & i & 0 \\ 0 & 0 & -2i \end{bmatrix}. \end{aligned} \tag{3}$$

With a rearrangement of order, this choice of $\mathfrak{su}(3)$ basis is seen to be equivalent to the Gell–Mann matrices [20]. In this basis, the Hamiltonian in (2) can be represented as

$$iH = -\Omega_{12}X_1 - \Omega_{23}X_2 - \frac{\Delta}{2}X_7 + \frac{\Delta}{2\sqrt{3}}X_8 + \frac{\Delta}{3}I_3 \tag{4}$$

where I_3 is the 3×3 identity matrix. We can drop the term $\Delta/3I_3$ since it commutes with all the other terms, and thus contributes only a global phase.

Without loss of generality, denote the spatial state of the left end and right end of the chain as

$$\rho_I = \begin{bmatrix} 1 & 0 & 0 \\ 0 & 0 & 0 \\ 0 & 0 & 0 \end{bmatrix} \quad \text{and} \quad \rho_T = \begin{bmatrix} 0 & 0 & 0 \\ 0 & 0 & 0 \\ 0 & 0 & 1 \end{bmatrix} \tag{5}$$

respectively. The electron shuttling can now be formulated as a steering problem, that is, for the dynamical system of (1), we will apply coherent tunneling amplitudes Ω_{12} and Ω_{23} as control fields to transfer the density matrix ρ from the initial state ρ_I at the initial time $t = 0$ to the final state ρ_T at the terminal time $t = T$.

In real experiments, the exact value of Δ can generally not be determined precisely, as a result of imperfections in materials and, for dopants in Si, inaccuracies intrinsic to the implantation techniques [6]. Instead, we may only know that the energy difference Δ lies in a range $[\Delta^* - \Delta_\epsilon, \Delta^* + \Delta_\epsilon]$, where Δ^* is the nominal value and Δ_ϵ is the maximum possible error bound. This is also the typical uncertainty that is encountered in engineering problems.

In the rest of this brief, we will design robust control pulses that can achieve the desired spatial state transfer regardless of what the true energy difference Δ is within the given range of uncertainty.

III. Robust Optimal Control Algorithm

To solve this robust state transfer problem, we shall sample a number of points in the uncertainty interval and then form a collection of state transfer problems, each of which has a different energy difference. We then apply a gradient algorithm to find the optimal solution that solves all these problems simultaneously.

Take N equally spaced points $\{\Delta_n\}_{n=1}^N$ in the uncertainty interval $[\Delta^* - \Delta_\epsilon, \Delta^* + \Delta_\epsilon]$, that is

$$\Delta_n = \Delta^* - \Delta_\epsilon + \frac{2(n-1)}{N-1}\Delta_\epsilon$$

and $\Delta_1 = \Delta^* - \Delta_\epsilon$, $\Delta_N = \Delta^* + \Delta_\epsilon$. For each Δ_n, we consider a dynamical system with the Liouville–von Neumann equation

$$\dot{\rho}_n = -[iH_n, \quad \rho_n] \tag{6}$$

where the Hamiltonian H_n is given by

$$iH_n = -\Omega_{12}X_1 - \Omega_{23}X_2 - \frac{\Delta_n}{2}X_7 + \frac{\Delta_n}{2\sqrt{3}}X_8. \tag{7}$$

We now have a set of N dynamical systems, which are all identical except for a different value of Δ in each case.

We want to steer all these N dynamical systems from the initial condition ρ_I to the final state ρ_T in (5). Denote the state trajectory of nth system as ρ_n. We can formulate the state transfer for this system as minimizing the cost function L_n, where $L_n = \|\rho_T - \rho_n(T)\|_F^2$. Here, the Frobenius norm is defined as $\|A\|_F^2 = \operatorname{Tr} AA^\dagger$. It is easy to show that $\operatorname{Tr} \rho_n(T)\rho_n^\dagger(T) = 1$, and we can derive that

$$L_n = 2 - 2 \operatorname{Tr} \rho_T \rho_n^\dagger(T).$$

Therefore, minimizing L_n amounts to maximizing the fidelity function $J_n = \mathrm{Tr}\,\rho_T \rho_n(T)$. The robust state transfer can now be formulated as maximizing the following aggregate fidelity of all the terminal states $\rho_n(T)$:

$$J = \sum_{n=1}^{N} \alpha_n J_n = \sum_{n=1}^{N} \alpha_n \,\mathrm{Tr}\,\rho_T \rho_n(T) \tag{8}$$

where α_n is a weighting factor that represents the probability that the uncertain parameter Δ takes a value close to Δ_n. In a typical scenario, we may have *a prior* knowledge that Δ is more probable to stay around the center of the uncertain range than the endpoints. In this case, we can choose a bell-shaped distribution for weighting factors α_n.

For the physical problem that we are interested, the coherent tunneling amplitudes Ω_{12} and Ω_{23} are used as control fields. In real physical experiments, there usually exist maximum frequency limits on the control signals. We, therefore, express the control fields as a finite summation of harmonics

$$\begin{aligned}\Omega_{12}(t) &= a_0 + \sum\nolimits_{m=1}^{M} [a_m \cos m\omega t + b_m \sin m\omega t] \\ \Omega_{23}(t) &= c_0 + \sum\nolimits_{m=1}^{M} [c_m \cos m\omega t + d_m \sin m\omega t]\end{aligned} \tag{9}$$

where $\omega = 2\pi/T$. Here, the expansions are truncated at a value M, which can be chosen so that $M\omega$ stays within the feasible frequency range. In the case when M is sufficiently large, (9) can approximate any continuous control function.

For time-varying control fields, there is generally no analytical method to solve the Liouville–von Neumann equation (6). To obtain numerical solutions, a common practice is to divide the total time duration into a number of small time steps and assume that the control functions are constant within each step. In particular, for a given time duration $[0, T]$, divide it into K equal intervals $\{[t_k, t_{k+1}]\}_{k=0}^{K-1}$ of length $\Delta t = t_{k+1} - t_k = T/K$, where $t_k = k\Delta t$. On each of these intervals $[t_k, t_{k+1}]$, assume the control fields in (9) take constant values, which are equal to those on the left boundary $t = t_k$

$$\begin{aligned}\Omega_{12}(k) &= a_0 + \sum\nolimits_{m=1}^{M} \left[a_m \cos mk\frac{2\pi}{K} + b_m \sin mk\frac{2\pi}{K}\right] \\ \Omega_{23}(k) &= c_0 + \sum\nolimits_{m=1}^{M} \left[c_m \cos mk\frac{2\pi}{K} + d_m \sin mk\frac{2\pi}{K}\right].\end{aligned} \tag{10}$$

From (7), we obtain

$$iH_n(k) = -\Omega_{12}(k)X_1 - \Omega_{23}(k)X_2 - \frac{\Delta_n}{2}X_7 + \frac{\Delta_n}{2\sqrt{3}}X_8. \tag{11}$$

Since $iH_n(k)$ is constant on the interval $[t_k,\ t_{k+1}]$, we can compute its unitary propagator as

$$U_n(k) = e^{-iH_n(k)\Delta t}. \tag{12}$$

It follows that the density operator at the final time can be calculated as:

$$\rho_n(T) = U_n(K-1)\cdots U_n(0)\rho_I U_n^{\dagger}(0)\cdots U_n^{\dagger}(K-1). \tag{13}$$

To realize the desired robust spatial state transfer, we now only need to maximize the aggregate fidelity in (8) with respect to the expansion coefficients a_m, b_m, c_m, and d_m in (9).

We now calculate the derivatives of the cost function J with respect to those expansion coefficients. For the ease of notation, let

$$\begin{aligned}\Omega_{12} &= \left[\Omega_{12}(0)\ \cdots\ \Omega_{12}(K-1)\right]^T \\ \Omega_{23} &= \left[\Omega_{23}(0)\ \cdots\ \Omega_{23}(K-1)\right]^T \\ p &= \left[a_0\ a_1\ \cdots\ a_M\ b_1\ \cdots\ b_M\right]^T \\ q &= \left[c_0\ c_1\ \cdots\ c_M\ d_1\ \cdots\ d_M\right]^T \\ \upsilon_K &= \left[0\ 1\ \cdots\ K-1\right]^T \quad \upsilon_M = \left[1\ \cdots\ M\right]^T.\end{aligned}$$

Then, the control fields in (10) can be rewritten in the following vector form:

$$\begin{aligned}\Omega_{12}(k) &= \left[1 \quad \cos\left(k\upsilon_M^T\frac{2\pi}{K}\right) \quad \sin\left(k\upsilon_M^T\frac{2\pi}{K}\right)\right] p \\ \Omega_{23}(k) &= \left[1 \quad \cos\left(k\upsilon_M^T\frac{2\pi}{K}\right) \quad \sin\left(k\upsilon_M^T\frac{2\pi}{K}\right)\right] q\end{aligned} \tag{14}$$

where the matrix functions $\cos(\cdot)$ and $\sin(\cdot)$ are calculated elementwise. Define

$$G = \left[\mathbf{1} \quad \cos\left(\upsilon_K\upsilon_M^T\frac{2\pi}{K}\right) \quad \sin\left(\upsilon_K\upsilon_M^T\frac{2\pi}{K}\right)\right]$$

where $\mathbf{1}$ is a column vector with all entries being one. Then, we have

$$\Omega_{12} = Gp, \quad \Omega_{23} = Gq. \tag{15}$$

The optimization variables thus become two vectors p and q, both of which lie in $\mathbb{R}^{M+1}$.

The closed-form formulas for dJ/dp and dJ/dq, i.e., the gradients of the aggregate fidelity J with respect to the expansion coefficient vectors p and q are given in the Appendix. With this, it is now straightforward to implement gradient types of algorithms [21].

IV. Numerical Optimization

In this section, we apply the gradients derived in the preceding section to design robust control fields that can realize the desired population transfer in solid-state devices.

We consider the ionized donor chain that was discussed in [2]. Typical values of the energy difference Δ are several megaelectronvolts, while the control fields Ω_{12} and Ω_{23} can be varied by $\pm 10^{-2}$ meV. Realistic parameter values allow us to assume a nominal value for Δ^* of 2.72 meV, with the actual value of Δ deviating from the nominal value by up to 20%. We further assume that the population transfer needs to be accomplished within 100 ns, and the maximum feasible frequency for control fields is 0.1 GHz. These constraints lead to the requirement that control field expansions in (10) need to be truncated at $M = 10$.

As a reference, we first consider the case with no robust design, i.e., optimizing for the point $\Delta = \Delta^*$ only. The corresponding population transfer and control fields are shown in Fig. 1(a) and (b), respectively. To test the robustness, we apply these control pulses to all 11 sampling points in the uncertainty range $[0.8\Delta^*, 1.2\Delta^*]$ meV. The results of these simulations are plotted in Fig. 2. It is evident that when the actual value of Δ is unknown within this range, the electron

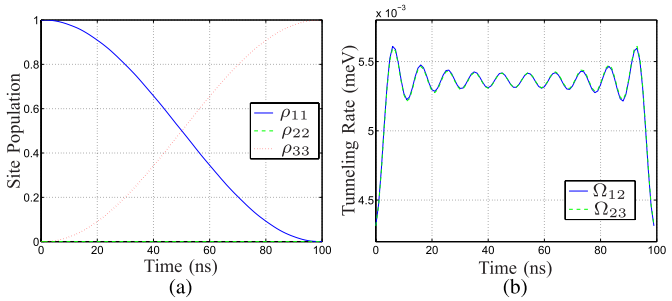

Fig. 1. Control pulses obtained with no robust design. (a) Spatial state transfer when $\Delta = \Delta^* = 2.72$ meV. (b) Control pulses: blue solid line corresponds to Ω_{12} and green dashed line to Ω_{23} (see electronic version for color plots).

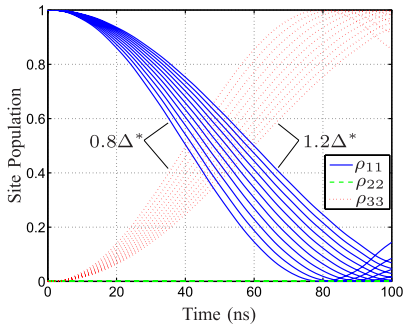

Fig. 2. Robustness test for the control pulses in Fig. 1: spatial state transfers for 11 evenly distributed Δ is in the range $[0.8\Delta^*, 1.2\Delta^*]$, where $\Delta^* = 2.72$ meV.

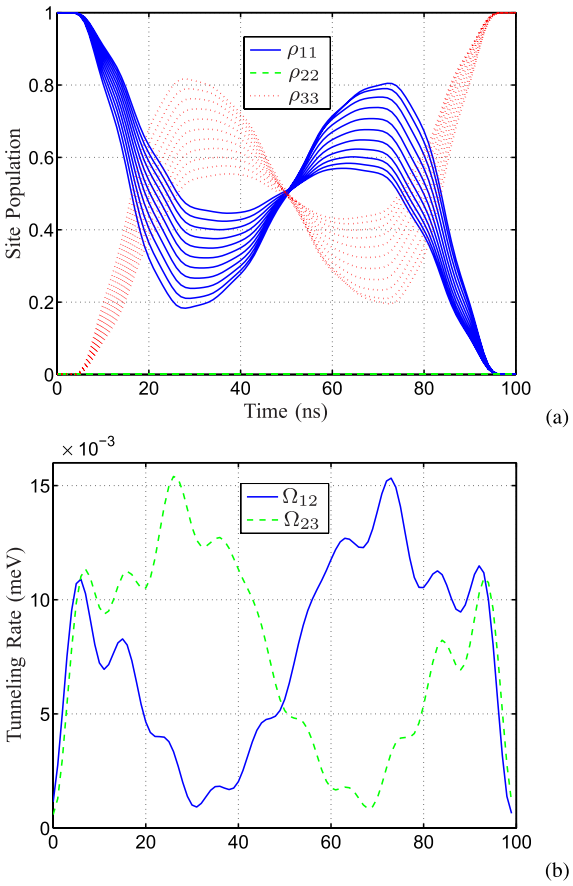

Fig. 3. Design of robust control fields. (a) Spatial transfer for 11 evenly distributed values of Δ is in the range $[0.8\Delta^*, 1.2\Delta^*]$, where $\Delta^* = 2.72$ meV. (b) Robust control pulses: blue solid line corresponds to Ω_{12} and green dashed line to Ω_{23} (see electronic version for color plots).

cannot be successfully transferred from left to right, except in the case when (coincidentally) $\Delta = \Delta^*$. Note that in each of the unsuccessful transfers, a full transfer is achieved at some point before the final time T. However, the oscillatory nature of the populations leads to a reversal of the transfer. Therefore, experimentally, a number of different transfer times would have to be attempted for a given pulse sequence in order to assess the possibility of a complete transfer and determine the optimal time. Furthermore, noise in any element of the Hamiltonian may cause the optimal transfer time for a given pulse sequence to be different for each individual experiment.

Next, we apply the robust control pulses design developed above. Discretize the total time duration $[0, 100]$ ns into 100 small time steps, each with length 1 ns. Let us take 11 evenly distributed sampling points Δ_n from the uncertainty range $[0.8\Delta^*, 1.2\Delta^*]$ meV. Further assume that we are certain that Δ is more probable to stay around the center of the uncertain range. We then choose the weighting factors as a bell-shaped function $\alpha_n = e^{(\Delta_n - \Delta^*)^2/\sigma^2}$, where $\sigma = (\Delta_1 - \Delta^*)^2/\log 10$. The parameter σ is chosen such that the weight at the center is one, whereas the weights at two endpoints are 0.1.

Given these parameter settings, we can apply a gradient algorithm with fixed step size to obtain the optimization results, as shown in Fig. 3. It is clear that whatever value of energy difference Δ within the $\pm 20\%$ deviation range of the nominal value $\Delta^* = 2.72$ meV is employed, the resulting robust control fields can transfer the population with almost perfect fidelity. Note that the population of ρ_{22} is close to zero at any point during the transfer. This is an advantage because it eliminates the decoherence associated with the middle site.

Moreover, the robust controls also yield the populations that do not oscillate when approaching the final time, as shown in Fig. 2. Slight changes in transfer time would, therefore, not affect the population transfer, a useful robustness feature from the experimental perspective. We also note these pulses perform well outside the range for which they were defined. For example, if the real uncertainty level is $\pm 25\%$ instead of $\pm 20\%$ in the design, the spatial state transfer still has acceptable performance, as shown in Fig. 4.

Now, we discuss some properties of the proposed robust control algorithm.

Remark 1: We have calculated the preceding numerical example for the sampling points from 2–14 in the uncertain range. It turns out that all these sampling points can yield almost perfect transfer fidelity, and hence reducing the number of sampling points has a little adverse affect on the robust performance of transferring the electron with uncertain parameter. In general, more sampling points require longer computational time and result in control pulses with larger energy cost. On the other hand, we observe that more sampling points generate control pulses that are more robust in the transfer time, that is, small variations in the terminal time will change only slightly the transfer fidelity.

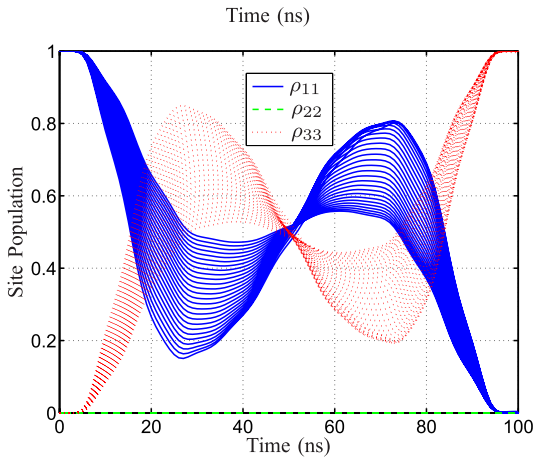

Fig. 4. Robustness test for ±25% uncertainty level: spatial state transfers for 26 evenly distributed Δ is in the range $[0.75\Delta^*, 1.25\Delta^*]$, where $\Delta^* = 2.72$ meV (see electronic version for color plots).

Remark 2: We have also run the numerical example for the values of M from 1–14. All these values of M can generate excellent control performance. In general, the larger M is, the higher transfer fidelity can be achieved. Nevertheless, we notice that even the case when $M = 1$, which corresponds to the control pulses consisting of only the first harmonics, can attain an average fidelity of 99.9940% over the uncertain range. This numerical study thus shows that robust control performance can be achieved even by a small number of M.

Remark 3: Different choices of weighting factors as well as unweighted case have been investigated. The numerical results show that all these cases generate close to perfect overall transfer fidelities, and the qualitative behavior of the resulting control pulses is similar. Further examinations of the fidelities achieved at each sampling points reveal that the sampling points with more weights can achieve even higher fidelity as expected. This makes it possible to better optimize for those more probable values of the uncertain parameters.

Remark 4: Define an energy type of cost as

$$\int_0^T \left(\Omega_{12}^2(t) + \Omega_{23}^2(t)\right)dt.$$

The energy cost for the case with no uncertainty in Fig. 1 is 0.0057, whereas that for robust control pulses in Fig. 3 is 0.0150. The robust pulses thus consume roughly 1.6 times more the energy than the ordinary ones. The additional energy required is the tradeoff to achieve the robust transfer for all the possible values in the uncertain range.

In a practical system, there usually exist hard constraints on the magnitudes of the control pulses. With the gradient calculations derived here, we can apply the sequential linear programming algorithm developed in [22] to deal with the constraints effectively.

V. Conclusion

In this brief, we have obtained robust control pulses designed for electron shuttling in a chain of donors, by formulating this as a collection of state transfer problems, each of which corresponds to a different value in the uncertainty parameter range. Writing the control signals in Fourier expansions allowed derivation of explicit formulas for the gradients of the aggregate fidelity with respect to Fourier coefficients. A direct gradient algorithm was then applied to solve this problem effectively. The results for electron shuttling across a three-site chain with uncertain values of intersite tunneling parameters show that the robust design significantly improves the performance of an electron shuttling protocol, achieving near perfect state transfer across a realistic range of Hamiltonian parameters for a phosphorus-doped silicon system. In the future, as noises are usually one of the major difficulties in solid-state devices, we plan to extend our approach to open system in a noisy environment.

Appendix
Derivation of Gradient

We derive here the gradients of the aggregate fidelity J with respect to p and q. From (8) and (15), we have

$$\frac{dJ}{dp} = \left(\frac{d\Omega_{12}}{dp}\right)^T \frac{dJ}{d\Omega_{12}} = G^T \sum_{n=1}^{N} \alpha_n \frac{dJ_n}{d\Omega_{12}}.$$

Similarly

$$\frac{dJ}{dq} = G^T \sum_{n=1}^{N} \alpha_n \frac{dJ_n}{d\Omega_{23}}.$$

Next, we derive $dJ_n/d\Omega_{12}(k)$ and $dJ_n/d\Omega_{23}(k)$. Define

$$\rho_n(k) = U_n(k-1)\cdots U_n(0)\rho_I U_n^\dagger(0)\cdots U_n^\dagger(k-1)$$
$$\Lambda_n(k) = U_n^\dagger(k)\cdots U_n^\dagger(K-1)\rho_T U_n(K-1)\cdots U_n(k)$$

where $U_n(k)$ is defined in (12), and $k = 0, \ldots, K-1$. In addition, define $\rho_n(0) = \rho_I$ and $\Lambda_n(K) = \rho_T$. Then

$$J_n = \mathrm{Tr}\,\Lambda_n(K)\rho_n(K) = \cdots = \mathrm{Tr}\,\Lambda_n(0)\rho_n(0).$$

It follows that:

$$\frac{dJ_n}{d\Omega_{12}(k)} = \mathrm{Tr}\,\Lambda_n(k+1) \times \left(\frac{dU_n(k)}{d\Omega_{12}(k)}\rho_n(k)U_n^\dagger(k) + U_n(k)\rho_n(k)\frac{dU_n^\dagger(k)}{d\Omega_{12}(k)}\right). \quad (16)$$

Using the following expression for the derivative of a matrix exponential [23]:

$$\frac{d}{d\upsilon}e^{-i(H_a+\upsilon H_b)t}\bigg|_{\upsilon=0} = -i\int_0^t e^{-iH_a\tau}H_b e^{iH_a\tau}d\tau\ e^{-iH_a t} \quad (17)$$

we obtain

$$\frac{dU_n(k)}{d\Omega_{12}(k)} = \int_0^{\Delta t} e^{-iH_n(k)\tau}X_1 e^{iH_n(k)\tau}d\tau\ U_n(k). \quad (18)$$

Substituting (18) into (16), we get

$$\frac{dJ_n}{d\Omega_{12}(k)} = \mathrm{Tr}\left[\rho_n(k+1), \Lambda_n(k+1)\right]\int_0^{\Delta t} e^{-iH_n(k)\tau}X_1 e^{iH_n(k)\tau}d\tau.$$

$$T_n(k) = \begin{bmatrix} -\Omega_{23}(k)/h(k) & \Omega_{12}(k)/\sqrt{g_n(k)(g_n(k)+\Delta_n)/2} & \Omega_{12}(k)/\sqrt{g_n(k)(g_n(k)-\Delta_n)/2} \\ 0 & -\sqrt{(g_n(k)+\Delta_n)/(2g_n(k))} & \sqrt{(g_n(k)-\Delta_n)/(2g_n(k))} \\ \Omega_{12}(k)/h(k) & \Omega_{23}(k)/\sqrt{g_n(k)(g_n(k)+\Delta_n)/2} & \Omega_{23}(k)/\sqrt{g_n(k)(g_n(k)-\Delta_n)/2)} \end{bmatrix}$$

We can further simplify this calculation. First note that since $H_n(k)$ is a Hermitian matrix, it can be diagonalized as

$$H_n(k) = T_n(k)\Gamma_n(k)T_n^\dagger(k) \tag{19}$$

where

$$\begin{aligned}\Gamma_n(k) &= \text{diag}\{\gamma_n^1(k), \gamma_n^2(k), \gamma_n^3(k)\} \\ &= \text{diag}\left\{-\frac{\Delta_n}{3}, \frac{\Delta_n + 3g_n(k)}{6}, \frac{\Delta_n - 3g_n(k)}{6}\right\}\end{aligned}$$

and the unitary matrix $T_n(k)$ can be written as, shown at the top of this page, and

$$\begin{aligned} g_n(k) &= \sqrt{\Delta_n^2 + 4\Omega_{23}^2(k) + 4\Omega_{12}^2(k)} \\ h(k) &= \sqrt{\Omega_{23}^2(k) + \Omega_{12}^2(k)}. \end{aligned}$$

Therefore, we can write

$$\begin{aligned}&\int_0^{\Delta t} e^{-iH_n(k)\tau} X_1 e^{iH_n(k)\tau} d\tau \\ &\quad = T_n(k) \int_0^{\Delta t} (T_n^\dagger(k) X_1 T_n(k)) \odot \Psi_n(k) d\tau \; T_n^\dagger(k) \end{aligned} \tag{20}$$

where $\odot$ denotes the Hadamard product, i.e., elementwise product, of two matrices, and the abth element of $\Psi_n(k)$ is $\exp\{i(\gamma_n^b(k) - \gamma_n^a(k))\tau\}$. Now, define a matrix $\Phi_n(k)$, whose abth element is given by

$$\Phi_n^{ab}(k) = \begin{cases} \dfrac{\exp\{i(\gamma_n^b(k) - \gamma_n^a(k))\Delta t\} - 1}{i(\gamma_n^b(k) - \gamma_n^a(k))}, & \text{for } a \neq b \\ \Delta t, & \text{for } a = b. \end{cases}$$

This allows (20) to be calculated explicitly

$$\begin{aligned}&\int_0^{\Delta t} e^{-iH_n(k)\tau} X_1 e^{iH_n(k)\tau} d\tau \\ &\qquad = T_n(k)((T_n^\dagger(k) X_1 T_n(k)) \odot \Phi_n(k)) T_n^\dagger(k)\end{aligned}$$

which in turn yields that

$$\begin{aligned}&\frac{dJ_n}{d\Omega_{12}(k)} \\ &\quad = \text{Tr}([\rho_n(k), \Lambda_n(k)] T_n(k)((T_n^\dagger(k) X_1 T_n(k)) \odot \Phi) T_n^\dagger(k)).\end{aligned}$$

A similar analysis leads to

$$\begin{aligned}&\frac{dJ_n}{d\Omega_{23}(k)} \\ &\quad = \text{Tr}([\rho_n(k), \Lambda_n(k)] T_n(k)((T_n^\dagger(k) X_2 T_n(k)) \odot \Phi) T_n^\dagger(k)).\end{aligned}$$

REFERENCES

[1] B. E. Kane, "A silicon-based nuclear spin quantum computer," *Nature*, vol. 393, no. 6681, pp. 133–137, 1998.

[2] A. D. Greentree, J. H. Cole, A. R. Hamilton, and L. C. L. Hollenberg, "Coherent electronic transfer in quantum dot systems using adiabatic passage," *Phys. Rev. B*, vol. 70, no. 23, p. 235317, 2004.

[3] B. Chen, W. Fan, and Y. Xu, "Adiabatic quantum state transfer in a nonuniform triple-quantum-dot system," *Phys. Rev. A*, vol. 83, no. 1, p. 014301, 2011.

[4] N. V. Vitanov, T. Halfmann, B. W. Shore, and K. Bergmann, "Laser-induced population transfer by adiabatic passage techniques," *Annu. Rev. Phys. Chem.*, vol. 52, pp. 763–809, Oct. 2001.

[5] J. Zhang, L. Greenman, X. Deng, and K. B. Whaley, "Optimal control for electron shuttling," *Phys. Rev. B*, vol. 62, p. 235324, Jun. 2013.

[6] T. Schenkel, C. Lo, C. Weis, A. Schuh, A. Persaud, and J. Bokor, "Critical issues in the formation of quantum computer test structures by ion implantation," *Nucl. Instrum. Methods Phys. Res. Section B, Beam Interactions Mater. Atoms*, vol. 267, no. 16, pp. 2563–2566, 2009.

[7] B. Koiller, X. Hu, and S. Das Sarma, "Exchange in silicon-based quantum computer architecture," *Phys. Rev. Lett.*, vol. 88, no. 2, p. 027903, 2001.

[8] D. Loss and D. P. DiVincenzo, "Quantum computation with quantum dots," *Phys. Rev. A*, vol. 57, no. 1, pp. 120–123, 1998.

[9] A. Doherty, J. Doyle, H. Mabuchi, K. Jacobs, and S. Habib, "Robust control in the quantum domain," in *Proc. 39th IEEE CDC*, vol. 1. Dec. 2000, pp. 949–954.

[10] H. Rabitz, "Control of quantum systems and inherent robustness to field fluctuations," in *Proc. 41st IEEE CDC*, vol. 1. Dec. 2002, pp. 441–443.

[11] M. A. Pravia *et al.*, "Robust control of quantum information," *J. Chem. Phys.*, vol. 119, no. 19, pp. 9993–10001, 2003.

[12] L. Viola and E. Knill, "Robust dynamical decoupling of quantum systems with bounded controls," *Phys. Rev. Lett.*, vol. 90, no. 3, p. 037901, Jan 2003.

[13] F. Ticozzi, A. Ferrante, and M. Pavon, "Robust steering of n-level quantum systems," *IEEE Trans. Autom. Control*, vol. 49, no. 10, pp. 1742–1746, Oct. 2004.

[14] C. D'Helon and M. R. James, "Stability, gain, and robustness in quantum feedback networks," *Phys. Rev. A*, vol. 73, no. 5, p. 053803, May 2006.

[15] J.-S. Li, "Ensemble control of finite-dimensional time-varying linear systems," *IEEE Trans. Autom. Control*, vol. 56, no. 2, pp. 345–357, Feb. 2011.

[16] K. Beauchard, P. S. P. da Silva, and P. Rouchon, "Stabilization for an ensemble of half-spin systems," *Automatica*, vol. 48, no. 1, pp. 68–76, 2012.

[17] J. A. V. Donkelaar *et al.*, "Top-down pathways to devices with few and single atoms placed to high precision," *New J. Phys.*, vol. 12, no. 6, p. 065016, 2010.

[18] C. J. Bradly, M. Rab, A. D. Greentree, and A. M. Martin, "Coherent tunneling via adiabatic passage in a three-well Bose-Hubbard system," *Phys. Rev. A*, vol. 85, p. 053609, May 2012.

[19] R. Rahman *et al.*, "Coherent electron transport by adiabatic passage in an imperfect donor chain," *Phys. Rev. B*, vol. 82, p. 155315, Oct. 2010.

[20] H. Georgi, *Lie Algebras In Particle Physics*, 2nd ed. Boulder, CO, USA: Westview Press, Oct. 1999.

[21] E. Polak, *Optimization: Algorithms and Consistent Approximations*. New York, NY, USA: Springer-Verlag, 1997.

[22] J. Zhang and R. Kosut, "Quantum potential design for electron transmission in semiconductor nanodevices," *IEEE Trans. Control Syst. Technol.*, vol. 21, no. 3, pp. 869–874, May 2012.

[23] I. Najfeld and T. F. Havel, "Derivatives of the matrix exponential and their computation," *Adv. Appl. Math.*, vol. 16, no. 3, pp. 321–375, 1995.